Electronic Supplementary Material (ESI) for Journal of Materials Chemistry

Graphene prepared via a novel pyridine-thermal strategy for capacitive deionization

Hui Wang, [a,b] Dengsong Zhang,*[a,b] Tingting Yan,[a] Xiaoru Wen,[a] Liyi Shi[a,b] and Jianping Zhang[b]

[a] *Research Center of Nano Science and Technology, Shanghai University, Shanghai 200444, China.*

Fax: 86 21 66134852; E-mail: dszhang@shu.edu.cn

[b] *Department of Chemistry, Shanghai University, Shanghai 200444, China.*

Experimental Section

Synthesis

All the chemicals were purchased from Sinopharm Chemical Reagent Company and used without further purification.

Graphite oxide (GO) was produced from nature graphite powders according to the reference[1]. The graphene (GR) was prepared as follows: in a typical experiment, the GO was firstly dispersed in a 40 mL of pyridine with a solid content of 8 mg/mL under the ultrasonication, and then a 40 mL of ethanol was added in the above dispersion. Subsequently, an 80mL portion of 4 mg/mL GO pyridine-ethanol was sealed in a 100 mL Teflon vessel, and maintained at 120^{o}C for 24h. Then the vessel was naturally cooled to room temperature. The products were washed by ethanol and deionized water several times, respectively. Finally, the products were dried at 60 ^{o}C for 24 h. For comparison, the GO was reduced by hydrazine according to the reference[2], and the product was denoted as GH.

Characterization

X-Ray diffraction (XRD) measurements were taken on a Rigaku D/MAX-RB X-ray diffractometer using Cu Kα radiation (40kV, 20 mA) and a secondary beam graphite monochromator. The morphologies were observed by transmission electron microscopy (TEM, JEOL JEM-200CX), and powdered samples were dispersed in ethanol by ultrasonication for 10 min in an ultrasonic bath. The morphologies were also

examined by field emission scanning electron microscopy (SEM, JEOL JSM-700F). An atomic force microscopy (AFM, Multimode Nanoscope IIIa) system was used to examine the surface characteristics of GR. The gas chromatography-mass spectrometry (GC-MS) was performed on the Agilent 7890A/5975C system. The analytes were separated by a HP-5MS capillary column of 30 m (0.25 i.d. and 0.25 mm film thickness), which was inserted directly into the ion source of the MS system.

Electrochemical measurements

The electrodes were prepared by mixing 90 wt% of GR and 10 wt% of polytetrafluoroethylene. The mixture was coated onto graphite paper and then the electrodes were dried at above 110 ^{o}C over night before the investigation of the total electrosorption capacity of GR.

The electrochemical performance of the electrodes was evaluated by cyclic voltammetry (CV) using a CHI 660D, carried out in a three-compartment cell including a GR electrode, a graphite, a saturated calomel electrode, which were used as the working, counter and reference electrodes, respectively. Here, the specific capacitances were obtained as the following equation:

$$C = \frac{\int IdV}{2\upsilon \Delta Vm} \qquad (1)$$

Electrochemical impedance spectroscopy (EIS) measurements were also measured by CHI 660D. The symmetrical cells are identical to the three-compartment cell mentioned above. The amplitude of the alternating voltage was 5 mV around the equilibrium potential (0 V); the data was collected in the frequency range from 10 mHz to 100 kHz.

The galvanostatic charge–discharge (GC) measurements were conducted on an automatic LAND battery test instrument to evaluate the charge/discharge performance in a 0.5 M NaCl aqueous solution.

Batch mode CDI experiments

The CDI performance of the electrodes was measured in a batch mode electrosorptive experiment, which was conducted in a continuous recycling system as shown in our previous publication[3]. The CDI electrodes were fabricated by mixing the

80 wt% of GR, 10 wt% of acetylene black and 10 wt% of polytetrafluoroethylene (5 wt% aqueous solution) homogenously. The ethanol was added into the mixture and then the slurry was pressed onto graphite sheets and dried at above 100^{o}C overnight. The size of the GR electrode is 50 mm × 60 mm × 0.3 mm. The CDI system herein included two sided electrodes separated by an insulated spacer. The NaCl aqueous solution with an initial conductivity of 86.9 μS cm^{-1} in a total volume of 20 mL was supplied to the cell using a pump with a flow rate of 25 mL min^{-1}. Meanwhile, the applied voltage was adjusted to 2.0 V and the electrode mass is 0.8g. The concentration change of the solution was measured by connecting a conductivity meter at the outlet of the cell, where the solution was released. Herein, the electrosorptive capacity of the electrode material was calculated according to the following equation:

$$S_C = \frac{(C_0 - C)V}{m} \qquad (2)$$

Where S_c is the electrosorptive capacity, C_0 and C are the initial and final concentrations, and V is the total volume of the NaCl aqueous solution. Meanwhile, m represents the total mass of the electrodes.

Additional Discussion

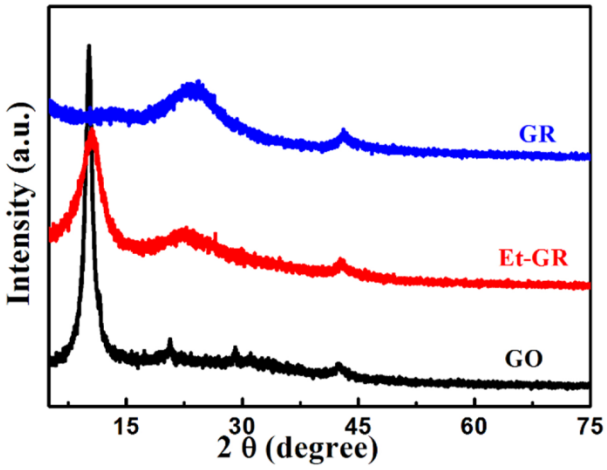

Figure S1.XRD patterns of GR, Et-GR (GO reduced in ethanol with the absence of pyridine) and GO

For comparison, the XRD pattern of Et–GR is shown in Figure S1. As seen obviously, the peak at 10.3^{o} still exist, indicating the reducing and exfoliate degree of

GO is compromised under the same experimental conditions in the absence of pyridine. During the reducing process, the partially reduced GR may re-agglomerate, and thus ethanol cannot pass into the deep region of GO. Therefore, the π-π stacking intercalation of pyridine molecules is favorable to the reduction of GO and the exfoliation of GR.

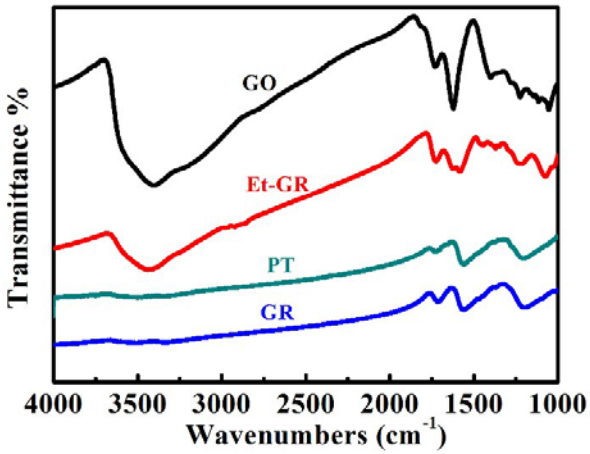

Figure S2. FT-IR spectra of GO, GR, Et-GR and PT (GO reduced in pyridine with the absence of ethanol).

Fig. S2 displays the FT-IR spectra of GO, GR, Et-GR and PT. In the spectrum of GO, a broad absorption band at 3400 cm^{-1}, is owing to stretching vibration of –OH. Two obvious peaks appear at 1735 and 1053$cm^{-1}$are due to –COOH and C-O. In contrast, after the pyridine-thermal reduction, the peak at 3400cm^{-1} was vanished, which reflects that GO has been reduced, so the hydrophile is decreased. Moreover, the bands at 1735 and 1053cm^{-1} almost disappear, indicating that most functional groups were removed[4]. In addition, we also investigated the reducing system in ethanol or pyridine. According the FT-IR spectrum of Et-GR, the intensities of the oxygen-containing groups is stronger than that of GR, which indicates that GO cannot be reduced completely by ethanol without pyridine. Interestingly, the peaks of oxygen-containing groups are also weakened in pyridine. In order to further discuss the effect of pyridine in the pyridine-thermal process, the reaction products were analyzed by the GC-MS. No oxidation product of pyridine was found in the pyridine system without ethanol, so we presume that oxygen-containing groups were removed due to the autogenous pressure and high temperature in the Teflon vessel[5]. In contrast, the oxidation products of

ethanol can be found in the GS-MS from the reaction system containing both ethanol and pyridine, and the product 1,1-Diethoxyethane formed under high temperature and pressure, which accounts for why ethanol accelerates the deep reduction of GO. In conclusion, high reduced GR products are yielded from the pyridine-thermal deoxygenization together with deep reduction from ethanol.

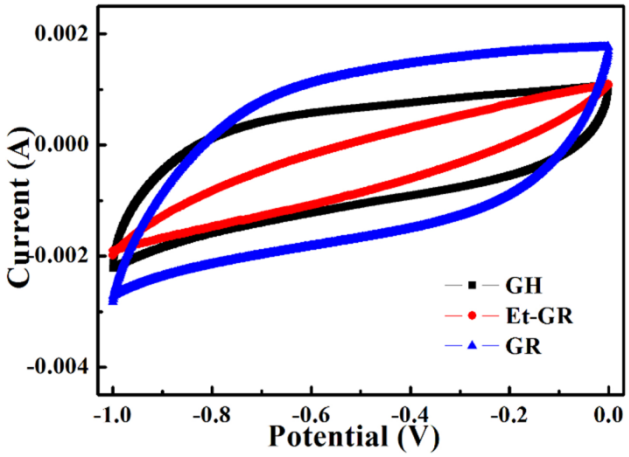

Figure S3. CV curves of Et-GR, GH and GR electrodes at a current density of 1 mVs^{-1} in a 0.5M NaCl aqueous solution

The CV curves of GR, GH and Et-GR are shown in Fig. S3. As calculated, it is clear that the special capacitance of the GR (115.1 F g^{-1}) is larger than that of Et-GR (33.5 F g^{-1}) or GH (74.8 F g^{-1}), indicating that the existence of pyridine in the reducing system is favorable to electrosorption performance of the electrodes. The strong intercalation of the pyridine molecules can improve the reduction and exfoliation efficiency of GR sheets, and the better exfoliation of the GR is beneficial to decreasing the inner resistance and increasing the conductivity of the as-prepared electrode. Therefore, the GR shows an excellent CV response.

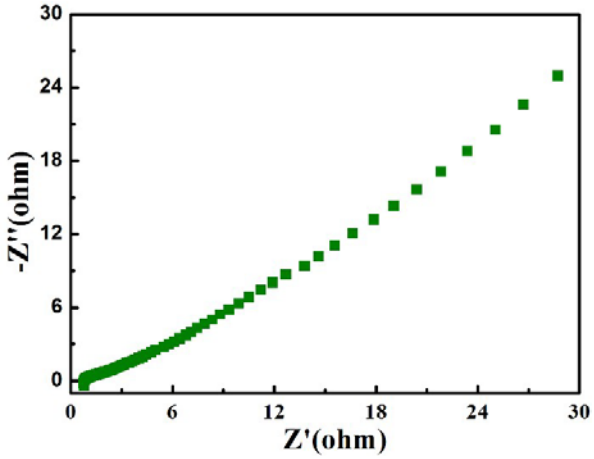

Figure S4. Nyquist impedance plots of GR in a 0.5 M NaCl aqueous solution.

The electrochemical impedance spectroscopy (EIS) of GR is shown in Fig. S4. As seen in the Nyquist impedance plots, the GR exhibits ideal capacitive behavior with a small semicircle at high frequency and an inclined line at low frequency. The deviated capacitor behavior in the low-frequency range is mainly due to the difficult accessibility of hydrated ions into certain pores of GR electrodes and the surface roughness[6, 7]. In addition, the low concentration of ions in the salty solution might partially contribute to the deviation in this case. The intersection point on the real axis at high frequency represents the equivalent resistance (ESR) including the resistance from electrodes, solution, and contact resistance between electrodes and current collectors. The impedance spectrum shows a low ESR, and indicates the GR has a low inter-resistance and a high conductivity, resulting in a lesser internal loss and a greater charge/discharge rate[8]. In other words, the method of pyridine-thermal strategy decreased the re-stacking of GR, which is beneficial for the diffusion of the salty ions onto the GR surface.

References

1. W. S. Hummers and R. E. Offeman, *J Am Chem Soc*, 1958, **80**, 1339–1339.
2. H. B. Li, T. Lu, L. K. Pan, Y. P. Zhang and Z. Sun, *J Mater Chem*, 2009, **19**, 6773-6779.
3. D. S. Zhang, X. R. Wen, L. Y. Shi, T. T. Yan and J. P. Zhang, *Nanoscale*, 2012, **4**, 5440-5446.
4. J. F. Shen, T. Li, Y. Long, M. Shi, N. Li and M. X. Ye, *Carbon*, 2012, **50**, 2134-2140.
5. C. Nethravathi and M. Rajamathi, *Carbon*, 2008, **46**, 1994-1998.
6. J. Gamby, P. L. Taberna P. Simon, J. F. Fauvarque and M. Chesneau, *J. Power Sources*, 2001, **101**, 109-116.
7. N. Brun, S. R. S. Prabaharan, C. Surcin, M. Morcrette, H. Deleuze, M. Birot, O. Babot, M.-F. Achard and R. Backov, *J Phys Chem C*, 2012, **116**, 1408-1421.

8. Z. Peng, D. S. Zhang, L. Y. Shi and T. T. Yan, *J Mater Chem*, 2012, **22**, 6603-6612.